

# Entrainment of solids in an internally circulating fluidized bed with draft tube

Young Tag Kim, Byung Ho Song<sup>1</sup>, Sang Done Kim<sup>\*</sup>

Department of Chemical Engineering and Energy and Environment Research Center, Korea Advanced Institute of Science and Technology, Taejon, 305-701, South Korea

Received 17 November 1995; accepted 14 July 1996

## Abstract

The effects of gas velocity and particle size  $d_p$  on the transport disengaging height (TDH) and solid entrainment rate  $E$  along the freeboard height were determined in a fluidized bed (0.3 m internal diameter by 2.6 m height) with or without a draft tube (0.1 m internal diameter by 0.3 m height). The entrainment rates of sand ( $d_p = 210\text{--}610\ \mu\text{m}$ ) and PVC ( $\bar{d}_p = 130\ \mu\text{m}$ ) particles along the axial height of the bed were measured by an isokinetic sampling probe. The entrainment rate in the freeboard region decreases exponentially with the freeboard height and the value at the bed surface increases sharply with increasing excess gas velocity ( $U - U_{mr}$ ) in the beds with or without a draft tube. The entrainment rate at the bed surface with a draft tube can be predicted by a correlation for conventional fluidized beds. The exponential decay coefficients  $a$  in the present and previous studies were correlated in terms of the Froude number and the ratio of gas velocities  $U_i/U$ . Also, the TDH values in the beds with and without a draft tube can be determined by  $\text{TDH} = (1/a)\ln(E_0/0.003)$ . © 1997 Elsevier Science S.A.

**Keywords:** Circulating fluidized bed; Entrainment rate; Transport disengaging height; Decay coefficients; Draft tube

## 1. Introduction

Circulating fluidized beds (CFB) have been employed widely in petroleum refining, coal combustion and gasification processes. However, conventional circulating fluidized beds require a very tall main vessel as a solids riser and accompanying tall cyclones. To reduce the height of a conventional CFB and the construction cost, several new types of CFB using a draft tube or flat plates to divide the bed for the circulation of internal solids in a single vessel have been developed [1,2]. Knowledge of the axial profile of the entrainment rate in the bed is required to design fluidized beds. Therefore, numerous studies have been carried out to determine the transport disengaging height (TDH) and solid entrainment rate  $E$  below the TDH, and several correlations have been proposed to predict TDH and  $E$  values in conventional fluidized beds [3–6]. However, studies on TDH and  $E$  in fluidized beds with a draft tube are very sparse. Therefore, in this study, the effects of gas velocity and particle size on TDH and  $E$  below the TDH were determined in a fluidized bed with and without a draft tube.

## 2. Experimental details

Experiments were carried out in a Plexiglas column of 0.3 m internal diameter (i.d.) by 2.5 m height with or without a centrally located draft tube (0.1 m i.d. by 0.3 or 0.6 m height) as shown in Fig. 1. The fluidized bed consisted of three parts: air box (0.3 m i.d.  $\times$  0.30 m high), main column (0.3 m i.d.  $\times$  1.7 m high) and an expanded freeboard section (0.45 m i.d.  $\times$  0.5 m high). The draft tube can be removed from the bed to make a conventional fluidized bed. The gap height, the distance between the distributor plate and the draft tube inlet, was adjusted to 0.14 m using three steel bars bolted on the draft tube. An annular shape distributor box was constructed to supply air into the draft tube and annulus independently. A distributor plate (0.1 m i.d.) with seven bubble caps (4 holes  $\times$  2.5 mm i.d. in each bubble cap) was used to introduce gas to the draft tube. Also, a conical plate having an inclined angle of 60° relative to the horizontal plane with 18 tuyeres (4 holes  $\times$  1.5 mm i.d. in each tuyere) was used for the annular gas supply. Details of the air box, distributor plate and tuyeres are shown in Fig. 2. Ten pressure taps were mounted flush with the column wall at 0.1 m height intervals from the distributor. The static pressures at the axial position of the fluidized bed were measured by liquid paraffin manometers. From the axial pressure profiles, the expanded bed

<sup>\*</sup> Corresponding author.

<sup>1</sup> Present address: Department of Chemical Engineering, KunSan National University, KunSan, Korea.

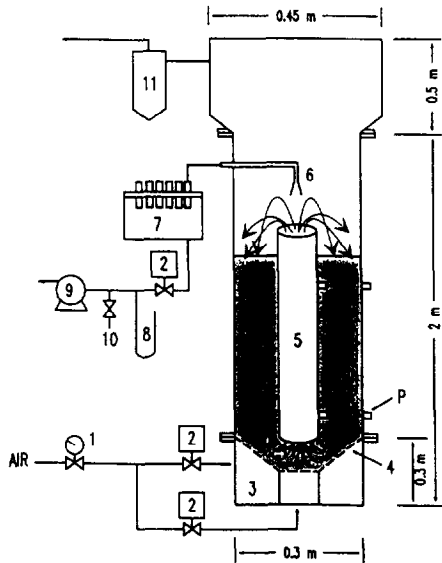


Fig. 1. Schematic diagram of the experimental apparatus: 1 pressure regulator, 2 flow meters, 3 air box, 4 gas distributor, 5 draft tube, 6 suction probe, 7 suction chamber, 8 water manometer, 9 vacuum pump, 10 bypass valve, 11 cyclone.

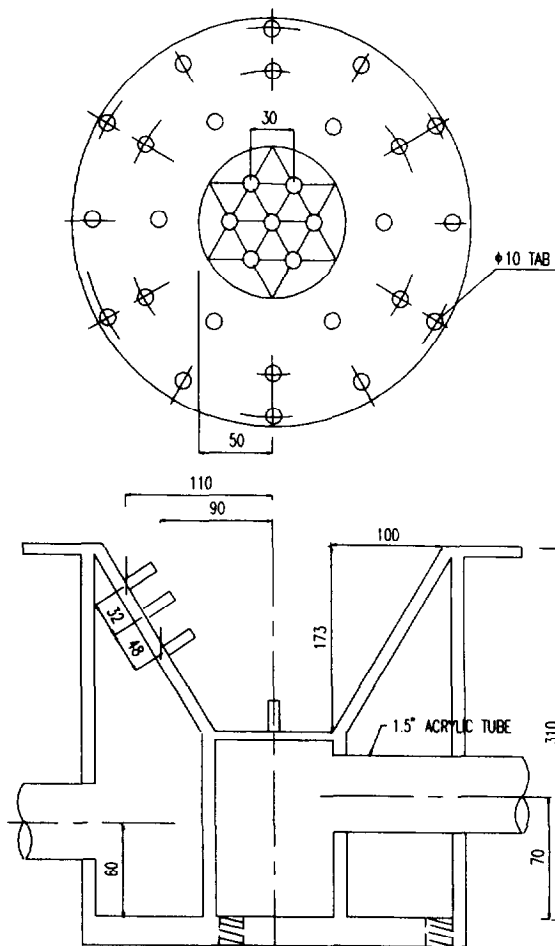


Fig. 2. Details of the air box, distributor and tuyeres.

height and bed density were determined. The initial static bed height was maintained at 0.40 m from the distributor plate. When using a draft tube, the expanded bed height was regarded as the distance between the distributor and the top

of the draft tube. To measure the concentration of entrained solids, ten sampling ports were mounted axially from the distributor at the column wall. The entrained solid particles were sampled through a conical shaped suction probe [7]. The diameter of the probe mouth (0.022 m i.d.) was reduced (0.012 m i.d.) in order to accelerate the solids and to prevent saltation in the sampling line. The particle loaded air passed into the paper filter thimbles where all the particles were trapped. The thimbles were enclosed in a suction chamber from which clean air was sucked by a vacuum pump. The air flow rate in the sampling line and the chamber pressure were measured by a flow meter and a water manometer respectively. To catch the entrained solid isokinetically, the suction flow rate of air through the probe mouth was maintained equal to the average superficial gas velocity in the bed. The entrainment rate was determined as the sampled solid mass for a given time (180 s) divided by the cross-sectional area of the bed. The entrainment rate at a given sampling height was determined by averaging the rates at three radial positions. The experimental and operating variables are listed in Table 1.

### 3. Results and discussion

#### 3.1. Axial profile of entrainment rate

The entrainment rates  $E$  of PVC particles along the freeboard height in the bed without or with a draft tube are shown in Figs. 3 and 4.  $E$  decreases markedly with the freeboard height and then remains essentially constant above TDH. Thus, the entrainment rate profile in the freeboard can be represented by the following equation [8], derived for a conventional fluidized bed:

$$E = E_{\infty} + (E_0 - E_{\infty}) \exp(-ah) \quad (1)$$

where  $E$ ,  $E_{\infty}$  and  $E_0$  are entrainment rates at a height  $h$  above the bed surface, above the TDH, and at the bed surface respectively.  $a$  is an exponential decay constant representing the characteristics of the fluidized bed system. Since  $E_{\infty}$  is found

Table 1  
Summary of the experimental conditions

Material	PVC	Sand
Mean particle diameter $\bar{d}_p$ ( $\mu\text{m}$ )	130	210, 270, 390, 460, 610
Mean density ( $\text{kg m}^{-3}$ )	1400	2620
Minimum fluidizing velocity ( $\text{m s}^{-1}$ )	0.008	0.04 ( $\bar{d}_p = 210 \mu\text{m}$ ), 0.06 ( $\bar{d}_p = 270 \mu\text{m}$ ), 0.12 ( $\bar{d}_p = 390 \mu\text{m}$ ), 0.17 ( $\bar{d}_p = 460 \mu\text{m}$ ), 0.27 ( $\bar{d}_p = 610 \mu\text{m}$ )
Air velocity ( $\text{m s}^{-1}$ )		without a draft tube $U = 0.32\text{--}0.55$ with a draft tube $U_d = 1.4\text{--}2.9$ , $U_s = U_{mf}$
Sampling height (m)		0.5, 0.65, 0.85, 1.05, 1.25, 1.45, 1.65, 1.85, 2.1, 2.3

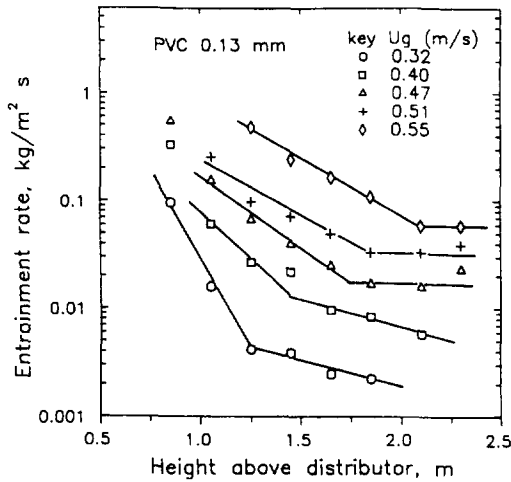


Fig. 3. Axial profile of entrainment rate in the fluidized bed without a draft tube.

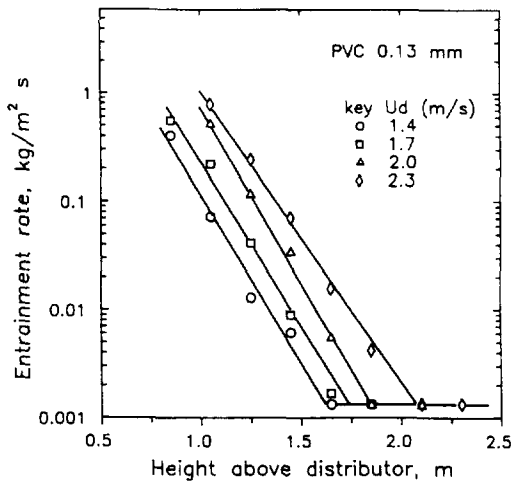


Fig. 4. Axial profile of entrainment rate in the fluidized bed with a draft tube.

to be very small compared with  $E_0$  in a bed of large particles such as in the present system, Eq. (1) can be simplified to

$$E = E_0 \exp(-ah) \quad (2)$$

### 3.2. Entrainment rate at the bed surface

It is known that solid particles are ejected into the freeboard owing to bubble eruption at the bed surface. When the bubbles burst at the bed surface, the upward momentum of the particles will carry particles into the freeboard. Therefore, particle carry-over from the bed surface depends on the mechanism of bubble eruption. Pemberton and Davidson [9] derived two approximate expressions for the particle entrainment rate at the bed surface based on the mechanisms of particle ejection from bubble roofs or wakes as

$$E_{Or} = 3d_p \rho_s (1 - \epsilon_{mf}) (U - U_{mf}) / D_b \quad (3)$$

$$E_{Ow} = 0.1 \rho_s (1 - \epsilon_{mf}) (U - U_{mf}) \quad (4)$$

where  $E_{Or}$  and  $E_{Ow}$  are the entrainment rate from the bubble roof and that from the bubble wake respectively.

The entrainment rate at the bed surface has been correlated [4] with the bubble size  $D_b$  and the excess gas velocity  $(U - U_{mf})$  as

$$\frac{E_0}{AD_b} = 3.07 \times 10^{-9} \frac{\rho_g^{3.5} g^{0.5}}{\mu^{2.5}} (U - U_{mf})^{2.5} \quad (5)$$

where  $D_b$  was estimated for the surface of the fluidized bed [10] as a function of superficial gas velocity  $U$ , expanded bed height  $H_e$ , the area of plate per hole  $A_0$  and column diameter  $D_t$  as

$$D_b = 0.474 \left( \frac{U - U_{mf}}{\phi \sqrt{g}} \right)^{0.4} (H_e + 3.94 \sqrt{A_0})^{0.8} \quad (6)$$

in which  $\phi = 0.64$  ( $D_t < 0.1$ );  $\phi = 1.6 D_t^{0.4}$  ( $0.1 \leq D_t < 1$ ). In the case of a fluidized bed with a draft tube,  $U = U_d$  since rising bubbles are confined to the draft tube.

The effect of gas velocity on  $E_0$  for sand (460  $\mu\text{m}$ ) and PVC (130  $\mu\text{m}$ ) particles with or without a draft tube is shown in Fig. 5 where  $E_0$  values are estimated by extrapolating the entrainment profile in the freeboard to the bed surface and compared with the calculated  $E_0$  values from Eqs. (3), (4) and (5). As can be seen,  $E_0$  values from the correlation of Pemberton and Davidson [3,9] exhibit much less depend-

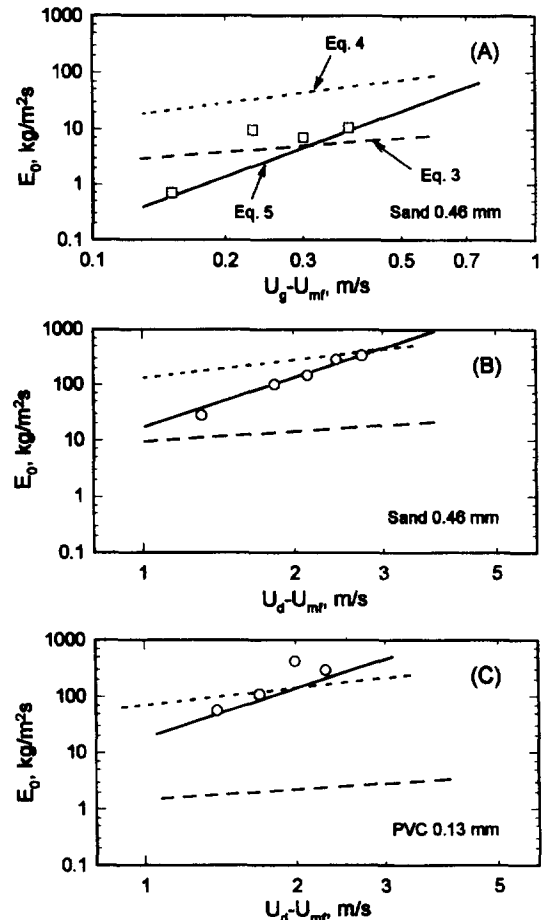


Fig. 5. The effect of gas velocity on the entrainment rate at the bed surface: (A) without draft tube; (B) and (C) with draft tube (— Eq. (5), ··· Eq. (4), --- Eq. (3)).

ence of  $E_0$  on gas velocity than the present and a previous study [5]. However, the correlation of Wen and Chen [4] predicts the experimental  $E_0$  values well for conventional fluidized beds. In a fluidized bed with a draft tube, gas streams are supplied to the draft tube and the annulus zones independently so that the draft tube zone can be operated in the slugging or turbulent flow regime and the annulus zone as a moving bed at the incipient fluidizing condition. Therefore, the entrainment rate at the annular bed surface can be regarded as zero and the draft tube zone is considered as a fluidized bed. Thus, the superficial gas velocity in the draft tube  $U_d$  is used as the gas velocity in the conventional fluidized bed and  $D_b$  is calculated based on the draft tube diameter in Eq. (6). Thus, the obtained  $E_0$  values are well in accord with the experimental data as shown in Fig. 4. Although Wen and Chen [4] recommended the use of column diameter instead of bubble diameter in a slugging fluidized bed,  $E_0$  can be predicted well from the bubble diameter rather than column diameter within the range of gas velocities employed in this study. The comparison between the calculated (Eq. (5)) and experimental values of  $E_0$  is shown in Fig. 6 in the bed with and without a draft tube.

### 3.3. Exponential decay coefficient $a$

The exponential decay coefficient is determined from the slopes of the log  $E$  vs.  $h$  plot. The variation of decay coefficients with the gas velocity through the draft tube ( $U_d$ ) and that through the main column ( $U$ ), is shown in Fig. 7 along with data from conventional fluidized beds [6,11]. As can be seen, the dependence of  $a$  on gas velocity in the present study is nearly same as in previous studies [6,11]. As can be seen in Fig. 6,  $a$  based on the total bed area rather than that of the draft tube for a fluidized bed with a draft tube is consistent with the coefficients in conventional fluidized beds.

It is known that the exponential decay coefficient is a function of gas velocity, particle size and bed diameter. Since there is no difference in freeboard geometry between the fluidized bed with and without a draft tube, the superficial

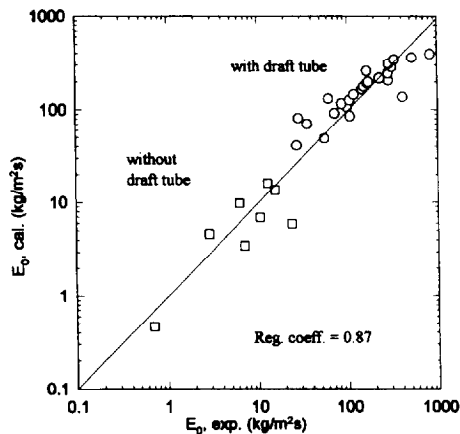


Fig. 6. Comparison of  $E_0$  between the experimental and calculated values from Eq. (5):  $\circ$  fluidized bed with draft tube,  $\square$  conventional fluidized bed.

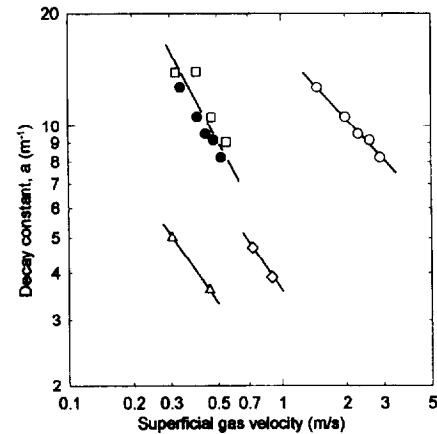


Fig. 7. Comparison of the experimental decay constants of 0.46 mm sand: with draft tube,  $\circ$  (based on  $U_d$ ),  $\bullet$  (based on  $U$ ); without draft tube  $\square$ ; Zenz and Weil [6]  $\triangle$ ; Bachovchin et al. [11]  $\diamond$ .

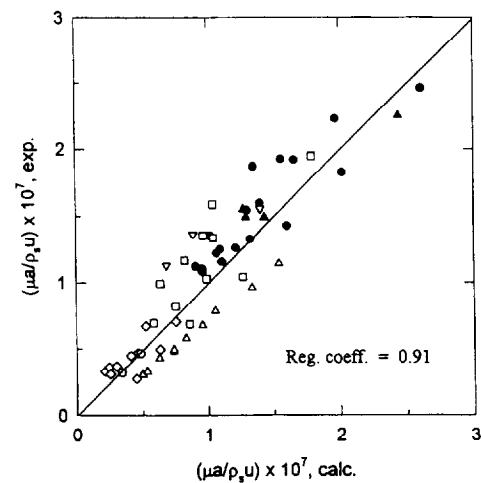


Fig. 8. Comparison of  $a$  between the calculated values from Eq. (7) and the experimental values:  $\circ$  Bachovchin et al. [11];  $\bullet$  this study (with draft tube);  $\square$  this study (without draft tube);  $\triangle$  Walsh et al. [12];  $\diamond$  Yoon et al. [7];  $\blacktriangle$  Large et al. [8];  $\nabla$  Zenz and Weil [6].

gas velocity through the total cross-section of the bed is used to determine the decay coefficient in the fluidized bed with a draft tube. Therefore, the constants  $a$  of the present and previous studies [6,8,10,12] have been correlated in terms of the Froude number and the ratio of the particle terminal velocity and superficial gas velocity as:

$$\frac{\mu a}{\rho_s U} = 3.8 \times 10^{-5} (U_t/U)^{-0.7} Fr^{-1} \quad (7)$$

with a correlation coefficient of 0.91 and a standard error of estimate of 0.19. The calculated values of  $a$  from Eq. (7) agree reasonably well with the experimental values in the literature [6–8,11,12] as shown in Fig. 8.

### 3.4. Transport disengaging height (TDH)

Variations of TDH with gas velocity in the bed with and without a draft tube are shown in Fig. 9 where TDH increases sharply with increasing gas velocity in conventional fluidized

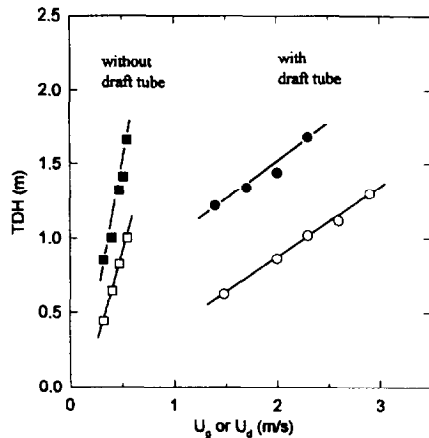


Fig. 9. Effect of gas velocity on TDH in a fluidized bed with and without a draft tube: ○ with draft tube, 0.46 mm sand; ● with draft tube, 0.13 mm PVC; □ without draft tube, 0.46 mm sand; ■ without draft tube, 0.13 mm PVC.

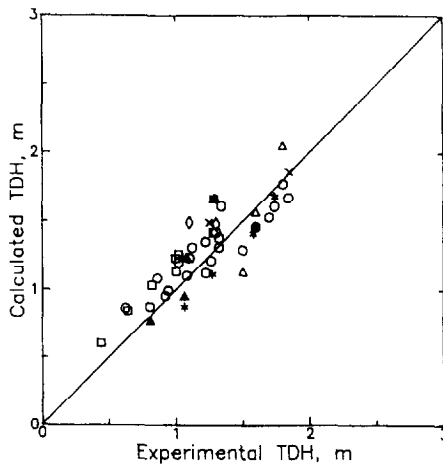


Fig. 10. Comparison between the experimental and calculated TDH from Eq. (9): ○ this study (with draft tube); □ this study (without draft tube); △ Nazemi et al. [14]; ▲ Yoon et al. [7]; ◇ Large et al. [8]; \* Horio et al. [15]; × Bachovchin et al. [11].

beds. However, the dependence of gas velocity on TDH in a fluidized bed with a draft tube is much lower than that in a conventional fluidized bed. Thus, solid entrainment in conventional fluidized beds can be reduced by introducing a draft tube in a conventional fluidized bed. In this study, the fluidized bed with a draft tube is divided into two regions: the dense bed and freeboard regions. Thus, Eq. (1) can be rearranged as

$$TDH = (1/a) \ln[(E_0 - E_\infty)/(E_{TDH} - E_\infty)] \quad (8)$$

where  $E_0$  can be calculated from Eq. (5) with bubble size at the bed surface and the  $E_\infty$  value is found to be near to zero in a bed of large particles. Also,  $a$  can be determined from Eq. (7) and the entrainment rate at the TDH can be assumed to be 1.0% of the entrainment rate at the bed surface [13]. However, TDH values so obtained are much lower than those of the present and previous [4] studies. Therefore, in this study, the mean value of the entrainment rate at TDH ( $0.003 \text{ kg m}^{-2} \text{ s}^{-1}$ ) is employed. Consequently, TDH values can

be determined by the following equation in the beds with and without draft tube:

$$TDH = (1/a) \ln(E_0/0.003) \quad (9)$$

where  $E_0$  and  $a$  can be determined from Eqs. (5) and (7). The TDH values predicted by the above equation are compared with the experimental values of the present and previous studies [7,8,11,14,15] as shown in Fig. 10.

#### 4. Conclusions

(1) The entrainment rate in the freeboard region decreases exponentially with freeboard height in the fluidized bed with or without a draft tube. (2) The fluidized bed with a draft tube has less dependence of TDH on gas velocity compared with the fluidized bed without a draft tube. (3) The entrainment rate at the bed surface with a draft tube can be predicted well by using the properly selected column diameter and gas velocity from a correlation proposed for conventional fluidized beds. The TDH values in both the fluidized beds with and without a draft tube can be estimated by the following equation:

$$TDH = (1/a) \ln(E_0/0.003)$$

#### 5. Nomenclature

$A$	Cross-sectional area of the bed ( $\text{m}^2$ )
$A_0$	Area of plate per hole ( $\text{m}^2$ )
$a$	Exponential decay constant in the entrainment equation ( $\text{m}^{-1}$ )
$D_b$	Bubble diameter near the bed surface (m)
$d_p$	Particle diameter (m)
$D_t$	Column diameter (m)
$E$	Entrainment rate of particles ( $\text{kg m}^{-2} \text{ s}^{-1}$ )
$E_0$	Entrainment rate at the bed surface ( $\text{kg m}^{-2} \text{ s}^{-1}$ )
$E_{0r}$	Entrainment rate ejected from bubble roofs ( $\text{kg m}^{-2} \text{ s}^{-1}$ )
$E_{0w}$	Entrainment rate ejected from the bubble wake ( $\text{kg m}^{-2} \text{ s}^{-1}$ )
$E_{TDH}$	Entrainment rate at the transport disengaging height ( $\text{kg m}^{-2} \text{ s}^{-1}$ )
$E_\infty$	Elutriation rate constant above TDH ( $\text{kg m}^{-2} \text{ s}^{-1}$ )
$Fr$	Froude number ( $U^2 g^{-1} d_p^{-1}$ )
$g$	Gravitational acceleration constant ( $\text{m s}^{-2}$ )

$H_e$	Expanded bed height (m)
$h$	Height above the dense bed surface (m)
$U$	Superficial gas velocity ( $\text{m s}^{-1}$ )
$U_a$	Superficial gas velocity to annulus ( $\text{m s}^{-1}$ )
$U_d$	Superficial gas velocity to draft tube ( $\text{m s}^{-1}$ )
$U_{mf}$	Minimum fluidizing gas velocity ( $\text{m s}^{-1}$ )
$U_t$	Terminal velocity of particle ( $\text{m s}^{-1}$ )

### 5.1. Greek letters

$\epsilon_{mf}$	Voidage at minimum fluidization condition
$\mu$	Gas viscosity ( $\text{kg m}^{-1} \text{s}^{-1}$ )
$\rho_g$	Density of gas ( $\text{kg m}^{-3}$ )
$\rho_s$	Density of solid particle ( $\text{kg m}^{-3}$ )
$\phi$	Constant in Eq. (6)

### Acknowledgements

We acknowledge a grant-in-aid for research from the Ministry of Trade, Commerce and Energy, Korea.

### References

- [1] W.C. Yang and D.L. Kearins, *Can. J. Chem. Eng.*, **61** (1983) 349.
- [2] R.D. LaNauze, *Powder Technol.*, **15** (1976) 117.
- [3] S.T. Pemberton and J.F. Davidson, *Chem. Eng. Sci.*, **41** (1986) 253.
- [4] C.Y. Wen and L.H. Chen, *AIChE J.*, **28** (1982) 117.
- [5] S.E. George and J.R. Grace, *Can. J. Chem. Eng.*, **59** (1981) 279.
- [6] F.A. Zenz and N.A. Weil, *AIChE J.*, **4** (1958) 472.
- [7] Y.S. Yoon, S.D. Kim and W.H. Park, *Korean J. Chem. Eng.*, **3** (1986) 121.
- [8] J.F. Large, Y. Martinie and M.A. Bergougnou, Interpretative model for entrainment in a large gas fluidized bed, *Int. Conf. on Powder Bulk Solids Handling and Processing, Rosemont, IL, 1976*, pp. 15–21.
- [9] S.T. Pemberton and J.F. Davidson, *Chem. Eng. Sci.*, **41** (1986) 243.
- [10] R.C. Darton, R.D. LaNauze, J.F. Davidson and D. Harrison, *Trans. Inst. Chem. Eng.*, **55** (1977) 274.
- [11] D.M. Bachovchin, J.M. Beer and A.F. Sarofim, *AIChE Symp. Ser.*, **77** (205) (1981) 76.
- [12] P.M. Walsh, J.E. Mayo and J.M. Beer, *AIChE Symp. Ser.*, **80** (234) (1984) 119.
- [13] I. Tanaka and H. Shinohara, *Int. Chem. Eng.*, **18** (1978) 276.
- [14] A. Nazemi, M.A. Bergougnou and C.G.J. Baker, *AIChE Symp. Ser.*, **70** (141) (1974) 98.
- [15] M. Horio, T. Shibata and I. Muchi, in D. Kunii and R. Toei (eds.), *Fluidization*, Engineering Foundation, New York, 1984, p. 307.